

Diboson and electroweak physics at ATLAS

A. VEST on behalf of the ATLAS COLLABORATION

Technische Universität - Dresden, Germany

ricevuto il 31 Luglio 2014

Summary. — LHC data at centre-of-mass energies of 7 and 8 TeV are used to perform measurements of electroweak diboson and Zjj production with the ATLAS detector. These measurements comprise combinations of W , Z and isolated photons, and use leptonic as well as semi-leptonic decay channels. No significant deviations from the Standard Model have been observed and the measurements are used to place constraints on anomalous gauge boson couplings. In addition, the prospects for vector boson scattering and triboson production at the LHC at a centre-of-mass energy of 14 TeV are discussed.

PACS 14.70.-e – Gauge bosons.

PACS 29.20.db – Storage rings and colliders.

1. – Introduction

Measurements of electroweak gauge boson pair production processes provide excellent tests of the electroweak sector of the Standard Model (SM). Any deviation from SM gauge constraints can cause a significant enhancement in the production cross section at high diboson invariant mass due to anomalous triple gauge boson couplings (aTGC). In the SM, triple gauge couplings (TGC) are predicted at tree level only with charged bosons, while neutral TGC are forbidden. Furthermore, diboson measurements are an evident prerequisite for the measurement of vector boson scattering, where dibosons plus at least two jets are produced.

This note presents measurements of the diboson and electroweak Zjj production cross sections in proton-proton collisions at centre-of-mass energies of $\sqrt{s} = 7$ TeV with an integrated luminosity of $L = 4.6 \text{ fb}^{-1}$ and at $\sqrt{s} = 8$ TeV with integrated luminosities of $L = 13 \text{ fb}^{-1}$ and 20 fb^{-1} , respectively, with the ATLAS [1] experiment. The cross sections of the studied processes are calculated at NLO in QCD using MCFM [2] with PDF set CT10 [3]. Furthermore, examples of limits on aTGC from the WW and the electroweak Zjj production measurement are given. In addition, the prospects for vector boson scattering and triboson production at the LHC at a centre-of-mass energy of $\sqrt{s} = 14$ TeV are discussed.

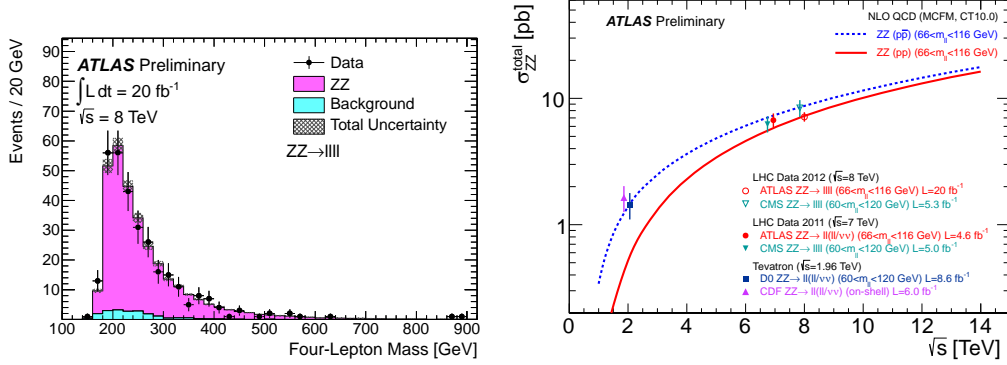


Fig. 1. – Left: The invariant mass of the four-lepton system for the ZZ selection. Right: Comparison of experimental measurements and theoretical predictions of the total ZZ production cross section as a function of the centre-of-mass energy \sqrt{s} . The solid red line shows the theoretical prediction for the ZZ production cross section in pp collisions, calculated using the natural width of the Z boson in the mass range 66 to 116 GeV.

2. – ZZ production

The analyses of Z boson pair production is performed in the $4l$ and $2l2\nu$ final states [4, 5]. The $ZZ \rightarrow llll$ signature comprises four isolated leptons and the invariant mass of each reconstructed opposite-sign same-flavor lepton pair forming a Z is required to be within $66 \text{ GeV} < m_{ll} < 116 \text{ GeV}$. For the $ZZ \rightarrow ll\nu\nu$ channel the signature is two opposite-sign same-flavor high p_T isolated leptons within $76 \text{ GeV} < m_{ll} < 106 \text{ GeV}$. Figure 1 (left) shows the invariant mass of the four-lepton system for the $ZZ \rightarrow llll$ selection. The total measured ZZ production cross sections are $\sigma_{\text{tot}} = 6.7 \pm 0.7(\text{stat})^{+0.4}_{-0.3}(\text{syst}) \pm 0.3(\text{lumi}) \text{ pb}$ for $\sqrt{s} = 7 \text{ TeV}$ and $\sigma_{\text{tot}} = 7.1^{+0.5}_{-0.4}(\text{stat}) \pm 0.3(\text{syst}) \pm 0.2(\text{lumi}) \text{ pb}$ for $\sqrt{s} = 8 \text{ TeV}$, and the theory predictions are $\sigma_{\text{tot}}^{\text{th}} = 5.89^{+0.22}_{-0.18} \text{ pb}$ and $\sigma_{\text{tot}}^{\text{th}} = 7.2^{+0.3}_{-0.2} \text{ pb}$ for $\sqrt{s} = 7 \text{ TeV}$ and 8 TeV , respectively. Figure 1 (right) illustrates the comparison of experimental measurements and theoretical predictions of the total ZZ production cross section as a function of the centre-of-mass energy.

3. – WZ production

The analysis of WZ production is performed with $3l\nu$ final states [6, 7]. The signature of these topologies is two opposite-sign same-flavor isolated leptons forming the Z boson within a tight invariant mass window around the Z pole of $|m_Z - m_{\text{PDG}}| < 10 \text{ GeV}$ which suppresses the background significantly. The residual third isolated lepton and the E_T^{miss} are forming the W boson. In fig. 2 (left) the transverse mass m_T of the W boson formed by the third lepton and E_T^{miss} is shown. The total WZ production cross section measurements are $\sigma_{\text{tot}} = 19.0^{+1.4}_{-1.3}(\text{stat}) \pm 0.9(\text{syst}) \pm 0.4(\text{lumi}) \text{ pb}$ for $\sqrt{s} = 7 \text{ TeV}$ and $\sigma_{\text{tot}} = 20.3^{+0.8}_{-0.7}(\text{stat})^{+1.2}_{-1.1}(\text{syst})^{+0.7}_{-0.6}(\text{lumi}) \text{ pb}$ for $\sqrt{s} = 8 \text{ TeV}$. The theory predictions are $\sigma_{\text{tot}}^{\text{theory}} = 17.6^{+1.1}_{-1.0} \text{ pb}$ and $\sigma_{\text{tot}}^{\text{theory}} = 20.3 \pm 0.8 \text{ pb}$ for $\sqrt{s} = 7 \text{ TeV}$ and 8 TeV , respectively. In fig. 2 (right) experimental measurements and theoretical predictions of the total WZ production cross section as a function of the centre-of-mass energy \sqrt{s} are compared. The total cross section is calculated using the natural width of the Z boson in the mass range 66 to 116 GeV.

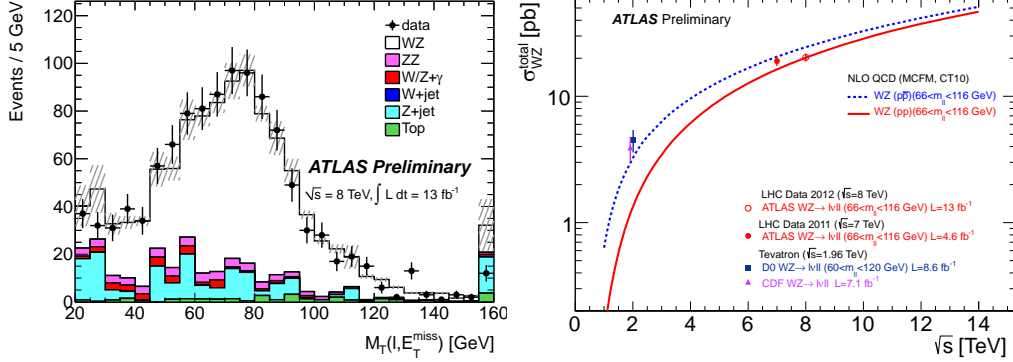


Fig. 2. – Left: The W transverse mass for the WZ selection. The rightmost bin includes the overflow. Right: Comparison of experimental measurements and theoretical predictions of the total WZ production cross section as a function of the centre-of-mass energy \sqrt{s} . The solid red line shows the theoretical prediction for the WZ production cross section in pp collisions, calculated using the natural width of the Z boson in the mass range 66 to 116 GeV.

4. – WW production

The $WW \rightarrow l\nu l\nu$ signal is measured in final states with two opposite-sign isolated leptons and large missing transverse energy [8]. Candidate WW events are required to have no jets reconstructed in the final state in order to reduce the background from $t\bar{t}$ production. The Z + jets processes with mis-measured jets are suppressed by a cut on E_T^{miss} . The measured total WW production cross section amounts to $\sigma_{\text{tot}} = 51.9 \pm 2.0(\text{stat}) \pm 3.9(\text{syst}) \pm 2.0(\text{lumi})$ pb compared to a theory prediction of $\sigma_{\text{tot}}^{\text{theory}} = 44.7_{-1.9}^{+2.1}$ pb, being slightly larger than the SM prediction. Figure 3 shows the normalized differential WW fiducial cross section as a function of the leading lepton p_T compared to the SM prediction.

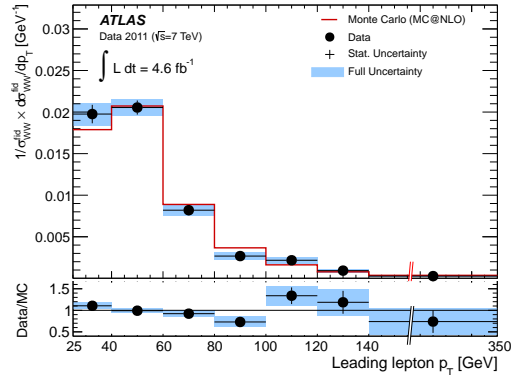


Fig. 3. – The normalized unfolded differential WW fiducial cross section as a function of the leading lepton p_T compared to the SM prediction.

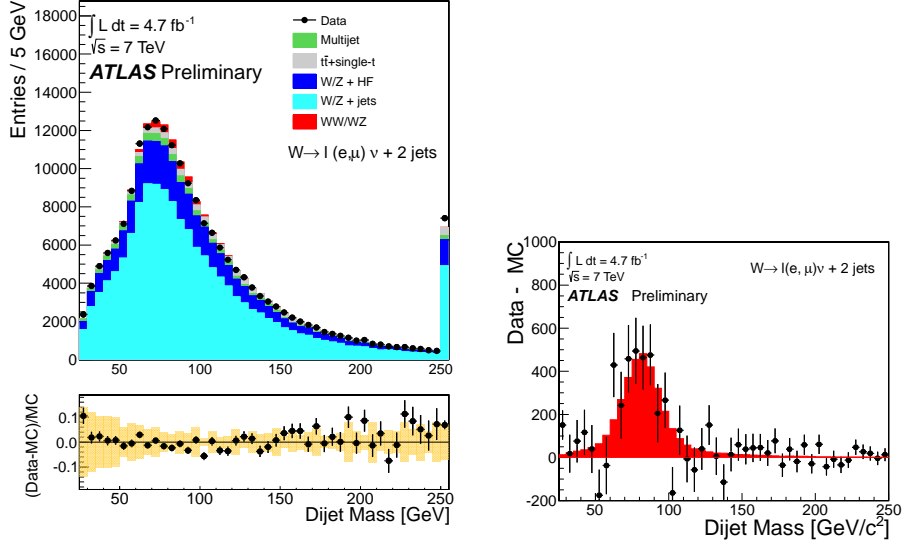


Fig. 4. – Left: dijet invariant-mass distribution of reconstructed $W/Z \rightarrow jj$ candidates. The rightmost bin includes the overflow. The lower panel displays the fractional difference between the data and the MC expectation. The yellow band displays the systematic uncertainty due to the JES uncertainty only. Right: Background-subtracted dijet invariant-mass distribution of reconstructed $W/Z \rightarrow jj$ candidates. The errors bars represents statistical uncertainty of data and MC.

5. – WW and WZ production in the single-lepton final state

WW and WZ production where one W or the Z boson decays into jets are also established [10] for $\sqrt{s} = 7$ TeV. Candidate events have one high p_T isolated lepton, $E_T^{\text{miss}} > 30$ GeV and exactly two jets with $p_T > 25/30$ GeV. Figure 4 shows the dijet invariant-mass distributions of reconstructed $W/Z \rightarrow jj$ candidates and the background-subtracted dijet invariant-mass distribution of reconstructed $W/Z \rightarrow jj$ candidates. The W/Z resonance has been observed with 3.3σ , and the measured cross section is $\sigma_{\text{tot}} = 72 \pm 9(\text{stat}) \pm 15(\text{syst}) \pm 13(\text{MC stat})$ pb, compared to the theory prediction of $\sigma_{\text{tot}}^{\text{theory}} = 63.4 \pm 2.6$ pb.

6. – $W\gamma$ and $Z\gamma$ production

The candidate events for production of W and Z bosons in association with photons are selected from the production processes $pp \rightarrow l\nu\gamma + X$, $pp \rightarrow ll\gamma + X$ and $pp \rightarrow \nu\nu\gamma + X$ [9]. The experimental signature comprises a high- p_T isolated photon and missing transverse energy for the $l\nu\gamma$ and $\nu\nu\gamma$ final states or two oppositely charged same-flavor leptons for the $ll\gamma$ final state. In order to suppress contributions from final-state radiation, the spacial separation between the lepton and the photon is required to be $\Delta R(l, \gamma) > 0.7$. Cross section measurements are performed in the inclusive and exclusive final state, depending on the number of jets produced. In fig. 5 the measured E_T^γ differential cross section for $pp \rightarrow W\gamma \rightarrow l\nu\gamma$ is shown for both the inclusive and exclusive measurements.

The resulting measured and expected inclusive and exclusive cross sections for $W\gamma$ and $Z\gamma$ production processes are compatible within uncertainties.

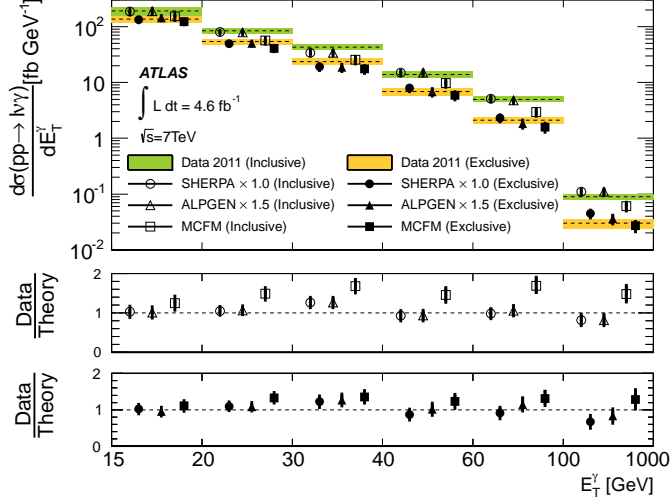


Fig. 5. – Measured E_T differential cross sections of the $pp \rightarrow l\nu\gamma$ process, using combined electron and muon measurements in the inclusive ($N_{\text{jet}} \geq 0$) and exclusive ($N_{\text{jet}} = 0$) extended fiducial regions.

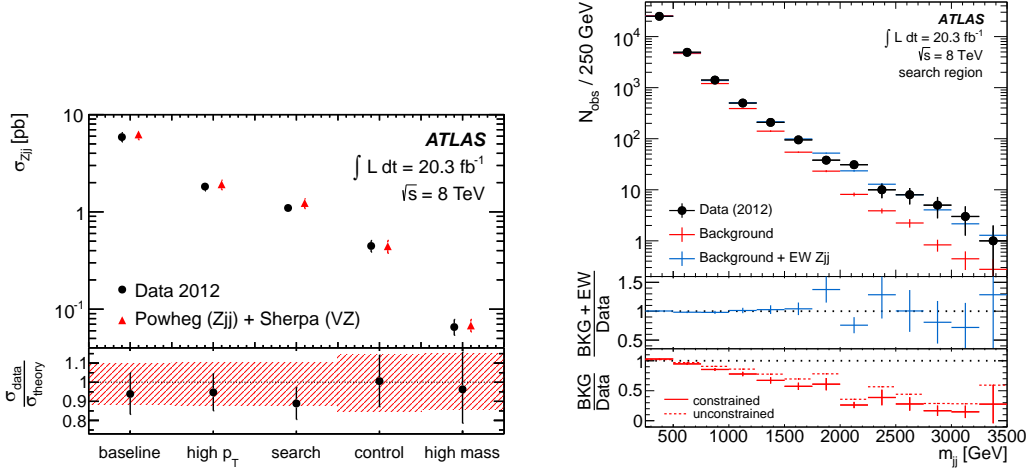


Fig. 6. – Left: Fiducial cross section measurements for inclusive Zjj production in the l^+l^- decay channel, compared to the POWHEG prediction for strong and electroweak Zjj production and the small contribution from diboson initiated Zjj production predicted by SHERPA [12]. Right: The dijet invariant-mass distribution in the search region. The signal and (constrained) background templates are scaled to match the number of events obtained in the fit. The lowest panel shows the ratio of constrained and unconstrained background templates to the data.

7. – Electroweak Zjj production

The three main electroweak Zjj production mechanisms are vector boson fusion (VBF), Z -boson bremsstrahlung, and non-resonant l^+l^-jj production and have been investigated with the 2012 dataset [11]. Candidate events have one opposite-sign same-

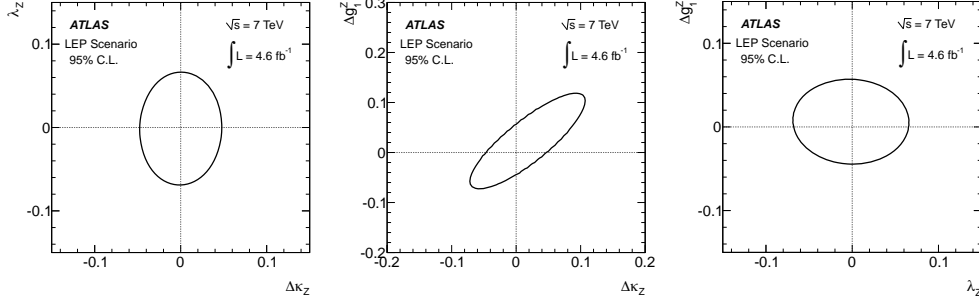


Fig. 7. – Two-dimensional 95% C.L. contour limit on λ_Z vs. $\Delta\kappa_Z$ (left), Δg_Z^1 vs. $\Delta\kappa_Z$ (middle), and Δg_Z^1 vs. λ_Z (right) for the LEP scenario for $\Lambda = \infty$. Except for the two parameters under study, all other anomalous couplings are set to zero.

flavor lepton pair within $81 \text{ GeV} < m_{ll} < 101 \text{ GeV}$ and at least two high- p_T jets. For the inclusive Zjj production a measurement of fiducial cross sections in five phase space regions with different sensitivity to the electroweak component have been performed, and are shown in fig. 6 (left). In the search regions the two highest- p_T jets (“tagging jets”) are required to fulfill $m_{jj} > 250 \text{ GeV}$ and 1 TeV , respectively. Additionally, a jet veto on additional jets in the rapidity interval between the two tagging jets is applied. The electroweak Zjj component is extracted using a two-component template fit to the m_{jj} spectrum. The background-only hypothesis could be rejected with a significance above the 5σ level. Figure 6 (right) shows the dijet invariant-mass distribution in the search region. The measured fiducial cross sections in the search region $m_{jj} > 250 \text{ GeV}$ is $\sigma_{\text{EW}} = 54.7 \pm 4.6(\text{stat})_{-10.4}^{+9.8}(\text{syst}) \pm 1.5(\text{lumi}) \text{ fb}$, compared to the theory prediction of $\sigma_{\text{theory}} = 46.1 \pm 0.2(\text{stat})_{-0.2}^{+0.3}(\text{scale}) \pm 0.8(\text{PDF}) \pm 0.5(\text{model}) \text{ fb}$.

8. – Exclusion limits on anomalous triple gauge couplings

The effect of physics beyond the Standard Model is modeled by an effective Lagrangian with anomalous triple gauge coupling (aTGC) parameters which are zero in the Standard Model [13, 14]. The five charged aTGC parameters are Δg_1^Z , $\Delta\kappa_Z$, $\Delta\kappa_\gamma$, λ_Z , and λ_γ . The eight neutral aTGCs parameters are h_3^Z , h_4^Z , h_3^γ , h_4^γ , f_4^Z , f_5^Z , f_4^γ , f_5^γ . In order to avoid unitarity violation, form factors $\mathcal{F}(s) = (1 + \hat{s}/\Lambda^2)^{-n}$ are used, where Λ is the scale of the form factor, \hat{s} is the effective centre-of-mass energy, and n is an arbitrary exponent. Figure 7 shows exemplary one- and two-dimensional confidence intervals at the 95% confidence level for the charged aTGC parameters derived from the WW production measurement [8] within the LEP parametrization, which defines $\Delta\kappa_Z = g_1^Z - \Delta\kappa_\gamma \tan \theta_w$ and $\lambda_Z = \lambda_\gamma$, and therewith reduces the number of independent parameters to three. No dipole form factor unitarization is used here. First ever aTGC limits at a hadron collider from VBF Z production, extracted from the search region $m_{jj} > 1 \text{ TeV}$ of the electroweak Zjj production measurement, with and without form factor unitarization are also derived [11].

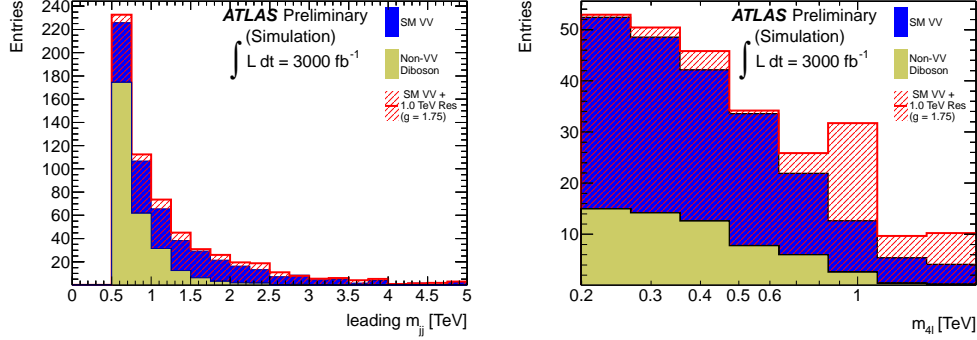


Fig. 8. – Left: Leading jet-jet invariant-mass (m_{jj}) distribution in the $pp \rightarrow ZZ + 2j \rightarrow lll + 2j$ channel. Right: Reconstructed 4-lepton mass (m_{4l}) spectrum for the $pp \rightarrow ZZ + 2j \rightarrow lll + 2j$ channel after requiring $m_{jj} > 1$ TeV.

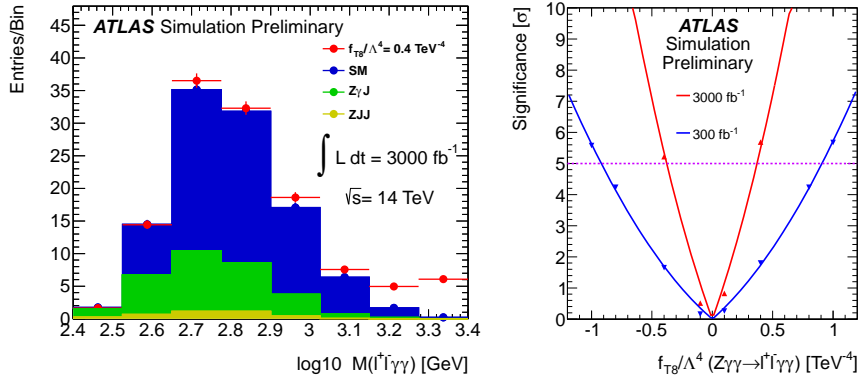


Fig. 9. – Left: Reconstructed mass spectrum of the $l^+l^-\gamma\gamma$ production process. Right: Signal significance as a function of f_{Ts}/Λ^4 .

9. – Prospects for vector boson scattering and triboson production at $\sqrt{s} = 14$ TeV

Vector boson scattering (VBS) is the key process to experimentally probe the nature of the mechanism of electroweak symmetry breaking. In VBS processes additional resonances of physics beyond the SM might show up. The signal investigated here is an anomalous VBS ZZ tensor singlet resonance f^0 with a resonance mass of $m = 1$ TeV, coupling $g = 1.75$, and width $\Gamma = 50$ GeV, and has been chosen as a benchmark [15, 16]. With an integrated luminosity of 3000 fb^{-1} this resonance could be observed with a significance of about 5.5σ . The studied signature is two opposite-sign, same-flavor lepton pairs, and at least two jets with $m_{jj} > 1$ TeV. Figure 8 shows for simulated events in the $pp \rightarrow ZZ + 2j \rightarrow lll + 2j$ channel the m_{jj} distribution (left) and the reconstructed 4-lepton mass spectrum (right).

Triboson production gives access to quartic gauge couplings, and the example discussed here is the $Z\gamma\gamma$ production [17]. Candidate events have two opposite-sign, same-

flavor high p_T leptons within the Z mass window of $|m_Z - m_U| < 10$ GeV, and two high- p_T well-separated photons. The expected sensitivity to anomalous $Z\gamma\gamma$ production at $\sqrt{s} = 14$ TeV in 5σ discovery values for the anomalous quartic gauge coupling parameters are $f_{T8}/\Lambda^4 = 0.4 \text{ TeV}^{-4}$ and $f_{T9}/\Lambda^4 = 0.7 \text{ TeV}^{-4}$ with an integrated luminosity of 3000 fb^{-1} . Figure 9 shows the reconstructed mass spectrum of the $l^+l^-\gamma\gamma$ production (left) and the signal significance as a function of f_{T8}/Λ^4 .

10. – Summary and conclusion

Measurements of electroweak diboson production with the ATLAS experiment continue to improve. Total and fiducial production cross section measurements of ZZ , WZ , WW , and $W/Z\gamma$ diboson production as well as electroweak Zjj production have been performed at a centre-of-mass energies of 7 TeV and/or 8 TeV. No significant deviations from the SM have been observed. Unfolded differential cross sections are available for all fully leptonic results at 7 TeV. The measured cross sections are consistent with the SM predictions, and limits on aTGC have been derived. Moreover, prospects for vector boson scattering and triboson production processes, which provide access to quartic gauge couplings, have been studied at a centre-of-mass energy of 14 TeV. An increase of significances for anomalous resonances or couplings with higher luminosity is expected.

REFERENCES

- [1] ATLAS COLLABORATION, *JINST*, **3** (2008) S08003.
- [2] CAMPBELL J. *et al.*, arXiv:1007.3492.
- [3] NADOLSKY P. M. *et al.*, *Phys. Rev. D*, **78** (2008) 013004.
- [4] ATLAS COLLABORATION, *JHEP*, **03** (2013) 128.
- [5] ATLAS COLLABORATION, ATLAS-CONF-2012-090, <https://cds.cern.ch/record/1460409>.
- [6] ATLAS COLLABORATION, *Eur. Phys. J. C*, **72** (2012) 2173.
- [7] ATLAS COLLABORATION, ATLAS-CONF-2013-021, <https://cdsweb.cern.ch/record/1525557>.
- [8] ATLAS COLLABORATION, *Phys. Rev. D*, **87** (2013) 112001.
- [9] ATLAS COLLABORATION, *Phys. Rev. D*, **87** (2013) 112003.
- [10] ATLAS COLLABORATION, ATLAS-CONF-2012-157, <https://cdsweb.cern.ch/record/1493586>.
- [11] ATLAS COLLABORATION, *JHEP*, **04** (2014) 031.
- [12] GLEISBERG T. *et al.*, *JHEP*, **0902** (2009) 007.
- [13] HAGIWARA K. *et al.*, *Nucl. Phys. B*, **282** (1987) 253.
- [14] ELLISON J. *et al.*, *Ann. Rev. Nucl. Part. Sci.*, **48** (1998) 33.
- [15] ATLAS COLLABORATION, ATL-PHYS-PUB-2012-005, <http://cds.cern.ch/record/1496527>.
- [16] ALBOTEANU A. *et al.*, arXiv:0806.4145.
- [17] ATLAS COLLABORATION, ATL-PHYS-PUB-2013-006, <http://cds.cern.ch/record/1558703>.